

RESEARCH ARTICLE

# Lack of robustness of textural measures obtained from 3D brain tumor MRIs impose a need for standardization

David Molina<sup>1\*</sup>, Julián Pérez-Beteta<sup>1</sup>, Alicia Martínez-González<sup>1</sup>, Juan Martino<sup>2</sup>, Carlos Velasquez<sup>2</sup>, Estanislao Arana<sup>3‡</sup>, Víctor M. Pérez-García<sup>1‡</sup>

**1** Mathematical Oncology Laboratory (MÓLAB), Universidad de Castilla-La Mancha, Ciudad Real, Spain, **2** Neurosurgery Department, Hospital Universitario Marqués de Valdecilla and Fundación Instituto de Investigación Marqués de Valdecilla, Santander, Spain, **3** Radiology Department, Fundación Instituto Valenciano de Oncología, Valencia, Spain

‡ Joint senior authors.  
\* [david.molina@uclm.es](mailto:david.molina@uclm.es)



**OPEN ACCESS**

**Citation:** Molina D, Pérez-Beteta J, Martínez-González A, Martino J, Velasquez C, Arana E, et al. (2017) Lack of robustness of textural measures obtained from 3D brain tumor MRIs impose a need for standardization. PLoS ONE 12(6): e0178843. <https://doi.org/10.1371/journal.pone.0178843>

**Editor:** Jonathan H Sherman, George Washington University, UNITED STATES

**Received:** March 22, 2017

**Accepted:** May 19, 2017

**Published:** June 6, 2017

**Copyright:** © 2017 Molina et al. This is an open access article distributed under the terms of the [Creative Commons Attribution License](https://creativecommons.org/licenses/by/4.0/), which permits unrestricted use, distribution, and reproduction in any medium, provided the original author and source are credited.

**Data Availability Statement:** Data are available at the following link: [https://figshare.com/articles/RESULTS\\_UPLOADED\\_xlsx/5001944](https://figshare.com/articles/RESULTS_UPLOADED_xlsx/5001944).

**Funding:** This work has been supported by Ministerio de Economía y Competitividad/FEDER, Spain [grant number MTM2015-71200-R], Consejería de Educación Cultura y Deporte from Junta de Comunidades de Castilla-La Mancha, Spain [grant number PEII-2014-031-P] and James S. Mc. Donnell Foundation 21st Century Science Initiative in Mathematical and Complex Systems

## Abstract

### Purpose

Textural measures have been widely explored as imaging biomarkers in cancer. However, their robustness under dynamic range and spatial resolution changes in brain 3D magnetic resonance images (MRI) has not been assessed. The aim of this work was to study potential variations of textural measures due to changes in MRI protocols.

### Materials and methods

Twenty patients harboring glioblastoma with pretreatment 3D T1-weighted MRIs were included in the study. Four different spatial resolution combinations and three dynamic ranges were studied for each patient. Sixteen three-dimensional textural heterogeneity measures were computed for each patient and configuration including co-occurrence matrices (CM) features and run-length matrices (RLM) features. The coefficient of variation was used to assess the robustness of the measures in two series of experiments corresponding to (i) changing the dynamic range and (ii) changing the matrix size.

### Results

No textural measures were robust under dynamic range changes. Entropy was the only textural feature robust under spatial resolution changes (coefficient of variation under 10% in all cases).

### Conclusion

Textural measures of three-dimensional brain tumor images are not robust neither under dynamic range nor under matrix size changes. Standards should be harmonized to use textural features as imaging biomarkers in radiomic-based studies. The implications of this

Approaches for Brain Cancer [Special Initiative Collaborative – Planning Grant 220020420 and Collaborative award 220020450]. The funders had no role in study design, data collection and analysis, decision to publish, or preparation of the manuscript.

**Competing interests:** The authors have declared that no competing interests exist.

work go beyond the specific tumor type studied here and pose the need for standardization in textural feature calculation of oncological images.

## Introduction

Textural analysis refers to a variety of mathematical methods used to quantify the spatial variations in grey levels within an image to derive the so-called ‘textural features’. These techniques have attracted much attention recently because of their potential use as imaging biomarkers [1], in part because of their connection with the concept of tumoral heterogeneity [2, 3]. Also, the emerging field of radiomics has used textural features, among other imaging features, as information proxies for characterizing tumors [4, 5, 6].

Many methods have been proposed to quantify tumor texture and heterogeneity from imaging data. First-order features quantify the grey level distribution accounting for the frequency of appearance of each grey level within the tumor [7]. Second-order textural features construct grey level relations between pairs of voxels. Co-occurrence matrix (CM) features [8] are one of the most used type of second order method.

On the other hand, run-length matrix (RLM) based features quantify the heterogeneity by measuring the distributions and area sizes (groups of connected voxels) within the tumor having similar grey level values, providing information on regional heterogeneity [9].

Texture characterization using CM and RLM-based methods has been extensively used in oncology [3, 6, 10, 11]. However, if textural features are to be used in clinical practice, they have to be robust under the typical variations found between different scanners, acquisition protocols, resolutions, etc [12].

The influence of the acquisition protocol on textural measures has been controversial in the literature and may depend on the specific parameter, tumors studied, etc [13, 14, 15, 16, 17]. Mayerhoefer et al. [13] and Waugh et al. [14] studied the influence of different clinical breast MRI protocols and parameters on the results of several textural features. They showed that spatial resolution is the most important factor influencing textural measures, while changes to other protocol parameters did not change the outcome of texture analyses so significantly. Collewet et al. [15] studied the effects of two MRI acquisition protocols and four image intensity normalization methods for texture classification. They found that the dynamic range discretization is also important for classification, as one of the four methods considered performed significantly better than the others. Leijenaar et al. [16] studied the variability of textural features in FDG PET images due to different acquisition modes and reconstruction parameters. Finally, Molina et al [17] found that many two-dimensional textural features were not robust under the combined effect of matrix size and dynamic range variation for a small set of patients.

To our knowledge most previous work has been focused on two-dimensional (2D) descriptors. However, it is already acknowledged that three-dimensional (3D) features are more representative of tumor properties and should be used instead [2, 18–20].

3D textural features have been less used in brain tumor imaging. Two studies have depicted their discrimination properties among VOIs containing metastases, gliomas and meningiomas [21]. Only a study has proven an increased performance of 3-D GLCMs compared to 2D in tumoral tissues classification [22].

The aim of this study was to analyze the robustness of the most common second order textural features used to characterize brain tumors in three-dimensional (3D) scenarios under changes of spatial resolution and dynamic range.

## Materials and methods

### Patients

67 patients with biopsy-proven glioblastoma were first considered for the study. The inclusion criterion was the availability of 3D pretreatment T1-weighted images. After that, in order to make sound analyses, we selected the most common image configuration and exclude the remaining patients. So, 20 patients ( $64.80 \pm 9.12$  years-old) were finally included in the study, that is, those with matrix of  $432 \times 432$  pixels and voxel size of  $0.5 \times 0.5 \times 1$  mm<sup>3</sup> (47 patients were finally excluded).

The study was approved by the Institutional Review Board (IRB) of Hospital Universitario Marqués de Valdecilla. Informed consent was waived by the IRB because we included only patients who had previously provided authorization for use of their medical records for research.

### Imaging protocol

All examinations were performed with a three-dimensional (3D) spoiled gradient recalled echo (SPGR). T1-weighted images of the whole brain without magnetization transfer were recorded after intravenous administration of a single-dose of gadobenate dimeglumine (0.1 mmol/kg, MultiHance, Bracco; Milan, Italy) with a 6-min delay.

Images were obtained using a 3-T magnet machine (Achieva, Philips Healthcare, Best, The Netherlands) with 22 cm field of view. Imaging parameters were: repetition time/echo time (TR/TE) of 20/11 ms; flip angle of 25°; matrix  $432 \times 432$  pixels, voxel size ( $0.5 \times 0.5 \times 1$  mm<sup>3</sup>).

### Image analysis

DICOM files were imported into the scientific software package Matlab (R2015b, The MathWorks, Inc., Natick, MA, USA) and processed using an in-house semi-automatic 3D image segmentation procedure [23]. Afterwards, segmented tumors were manually corrected.

### Textural analysis

A set of textural quantities derived from co-occurrence (CM) and run-length matrices (RLM) were chosen for this study and computed for tumors after segmentation.

The CM is a square matrix with dimension equal to the number of grey levels present in the image (dynamic range). It measures the relations between pairs of voxels within an image (8). It is usually characterized by a distance between pixels (e.g. adjacent pixels, pixels having at least one common neighbor, etc.) and one angle/direction (0°, 45°, 90°, 135°). Changing the distance or the direction leads to different matrices. Many previous studies have constructed different co-occurrence matrices by combining these parameters. However, in oncological imaging a more straightforward workflow is to obtain an averaged CM matrix considering every possible direction, i.e. the relations between each voxel and its 26 neighbors in 3D [20, 24]. In this work only the 3D CM was developed, providing more robust measurements. Also, we considered unit distance to construct our CM. Thus, each cell  $CM(i,j)$  in the CM matrix corresponds to the number times that one voxel of intensity  $i$  is a neighbor of another voxel with intensity  $j$  in 3D. Most common features derived from the CM were the Entropy,

Homogeneity, Contrast, Dissimilarity and Uniformity [7, 25]. For a comprehensive description of the meaning of each of the CM-based measures see Kurani et al [26].

The RLM matrix constructed in this work follows the same principles used for the CM. Thus, each cell  $RLM(i,j)$  was constructed as the number of runs of length  $j$  formed by voxels of intensity in box  $i$  considering all the 13 possible 3D directions [24, 27]. It is interesting to point out that this kind of textural analysis allows for a better characterization of tumor heterogeneity, being able to describe complex 3D structures labeled with the same grey level values. Most popular textural features based on the RLM were the Long Run Emphasis (LRE), Short Run Emphasis (SRE), Low Grey level Run Emphasis (LGRE), High Grey level Run Emphasis (HGRE), Short Run Low Grey level Emphasis (SRLGE), Short Run High Grey level Emphasis (SRHGE), Long Run Low Grey level Emphasis (LRLGE), Long Run High Grey level Emphasis (LRHGE), Grey level Non-Uniformity (LRHGE), Grey level Non-Uniformity (GLNU), Run-Length Non-Uniformity (RLNU) and Run Percentage (RPC) [27]. An intuitive description of the meaning of the RLM measures considered was done by Xu et al [28].

Further details on the measures definition can be found in Table 1.

The construction of the CM and RLM depends on the spatial resolution and dynamic range considered. Two different matrix sizes were used in this work: 432x432 (raw matrix) and 256x256 (standard MRI matrix size). The latter was obtained by interpolation using the Matlab software (v. R2016b) on the raw images. Also, we considered two different resolutions along z-axis: 1 mm (raw) and 2 mm (also obtained by interpolation on each pair of initial slices). For these four combinations of spatial resolutions, we discretized the dynamic range in 16, 32 and 64 different grey levels, as these are the most used and recommended dynamic ranges for these measures [17]. This procedure led to 12 different datasets for each patient.

Fig 1 shows an example of six resized and discretized slices obtained from the same tumor, using 432x432, 256x256 as matrix sizes and 16, 32 and 64 as dynamic ranges.

Finally, a set of 5 CM and 11 RLM heterogeneity textural features were computed for each image configuration using the Matlab software. Table 1 shows the mathematical expression of each textural parameter computed in this study.

## Robustness evaluation

Once the textural features were computed, robustness was assessed by means of the coefficient of variation (CV) [29]. The CV is a standardized measure of dispersion which is defined as the ratio between the standard deviation and the mean of a series of data. The result is typically reported as a percentage.

The mean of the CVs was obtained for all patients included. Textural features with a mean CV smaller than 10% were considered to be robust.

## Results

We computed the features listed in Table 1 for each of the 20 patients and each combination of spatial resolution and dynamic range considered leading to a total of 3840 textural feature values. With these data we performed several comparisons, which are discussed below.

### Experiment 1. Consistency of spatial resolutions for varying dynamic ranges

For each textural feature, patient and spatial resolution, we computed the CV using data for dynamic ranges of 64, 32 and 16 grey levels. This parameter provided a measure of the dependence of the textural features under changes of the grey levels. Then, the mean value and the standard deviation for the set of 20 patients included in the study were computed.

**Table 1. Textural features considered in this study.**

Type of measure	Name	Formula
Co-occurrence matrix	Entropy	$-\sum_{i=1}^N \sum_{j=1}^N CM(i,j) \cdot \ln[CM(i,j)]$
Co-occurrence matrix	Homogeneity	$\sum_{i=1}^N \sum_{j=1}^N \frac{CM(i,j)}{1 + (i-j)^2}$
Co-occurrence matrix	Contrast	$\sum_{i=1}^N \sum_{j=1}^N CM(i,j) \cdot (i-j)^2$
Co-occurrence matrix	Dissimilarity	$\sum_{i=1}^N \sum_{j=1}^N CM(i,j) \cdot  i-j $
Co-occurrence matrix	Uniformity	$\sum_{i=1}^N \sum_{j=1}^N [CM(i,j)]^2$
Run-length matrix	Long Run Emphasis (LRE)	$\frac{1}{n_r} \sum_{i=1}^N \sum_{j=1}^M RLM(i,j) \cdot j^2$
Run-length matrix	Short Run Emphasis (SRE)	$\frac{1}{n_r} \sum_{i=1}^N \sum_{j=1}^M \frac{RLM(i,j)}{j^2}$
Run-length matrix	Low Grey-level Run Emphasis (LGRE)	$\frac{1}{n_r} \sum_{i=1}^N \sum_{j=1}^M \frac{RLM(i,j)}{i^2}$
Run-length matrix	High Grey-level Run Emphasis (HGRE)	$\frac{1}{n_r} \sum_{i=1}^N \sum_{j=1}^M RLM(i,j) \cdot i^2$
Run-length matrix	Short Run Low Grey-level Emphasis (SRLGE)	$\frac{1}{n_r} \sum_{i=1}^N \sum_{j=1}^M \frac{RLM(i,j)}{i^2 \cdot j^2}$
Run-length matrix	Short Run High Grey-level Emphasis (SRHGE)	$\frac{1}{n_r} \sum_{i=1}^N \sum_{j=1}^M \frac{RLM(i,j) \cdot i^2}{j^2}$
Run-length matrix	Long Run Low Grey-level Emphasis (LRLGE)	$\frac{1}{n_r} \sum_{i=1}^N \sum_{j=1}^M \frac{RLM(i,j) \cdot j^2}{i^2}$
Run-length matrix	Long Run High Grey-level Emphasis (LRHGE)	$\frac{1}{n_r} \sum_{i=1}^N \sum_{j=1}^M RLM(i,j) \cdot i^2 \cdot j^2$
Run-length matrix	Grey-Level Non-Uniformity (GLNU)	$\frac{1}{n_r} \sum_{i=1}^N \left( \sum_{j=1}^M RLM(i,j) \right)^2$
Run-length matrix	Run-Length Non-Uniformity (RLNU)	$\frac{1}{n_r} \sum_{j=1}^M \left( \sum_{i=1}^N RLM(i,j) \right)^2$
Run-length matrix	Run Percentage (RPC)	$\frac{n_r}{\sum_{i=1}^N \sum_{j=1}^M RLM(i,j) \cdot j}$

Definition of the textural features considered in this study. For co-occurrence (CM) measures CM(i,j) stands for the co-occurrence matrix, N is the number of classes of grey-levels taken (8, 16, 32 and 64 in this study). For run-length matrix (RLM) measures RLM(i,j) is the run-length matrix, n<sub>r</sub> is the number of runs, N is the number of classes of grey-levels and M is the size in voxels of the largest region found.

<https://doi.org/10.1371/journal.pone.0178843.t001>

Table 2 shows the results for the mean values obtained for the whole set of patients and the standard deviations, both in percentages. No measure was found to be robust (mean CV smaller than 10%) under the variation of the dynamic range.

The same result was found when patients were considered individually instead of the means. For example, in Fig 2 we plot the normalized values of four relevant textural measures

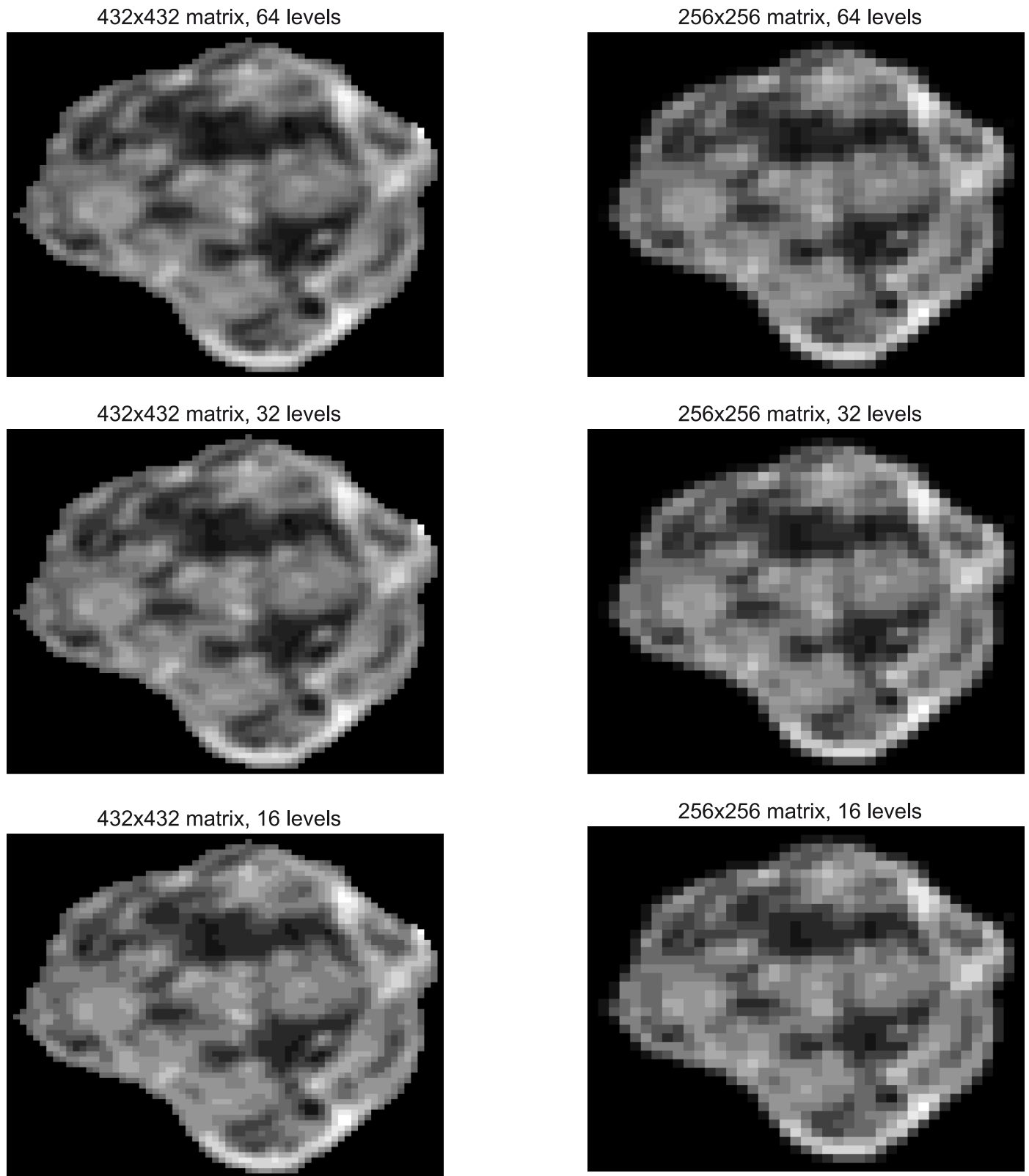


**Fig 1. Resized and discretized images for the same slice using 432x432 and 256x256 as matrix sizes and 64, 32 and 16 as dynamic ranges.** Running title of each image identifies the matrix size and dynamic range considered.

<https://doi.org/10.1371/journal.pone.0178843.g001>

**Table 2. Mean (and standard deviation) of the CV computed for the 20 patients.** Results are shown for each combination of spatial resolution and slice thickness considered. CV was computed for each feature considering different dynamic range values, i.e. 16, 32 and 64 grey levels.

		Matrix size and slice thickness			
		432x432; 1 mm	432x432; 2 mm	256x256; 1 mm	256x256; 2 mm
Co-occurrence matrix	Entropy	34.66 (6.42)	32.74 (5.04)	32.12 (5.65)	31.67 (5.23)
	Homogeneity	24.06 (3.99)	25.63 (3.95)	29.57 (4.12)	31.07 (4.43)
	Contrast	105.68 (5.25)	108.84 (3.25)	111.29 (1.52)	111.55 (1.49)
	Dissimilarity	66.17 (3.20)	65.80 (1.65)	66.50 (2.22)	66.50 (1.85)
	Uniformity	99.20 (9.25)	99.86 (10.01)	101.49 (9.82)	102.28 (10.38)
Run-length matrix	LRE	152.94 (11.34)	157.68 (10.91)	155.25 (9.34)	159.50 (9.92)
	SRE	13.11 (23.75)	15.16 (15.16)	12.89 (5.88)	23.41 (16.33)
	LGRE	94.26 (18.56)	105.25 (16.39)	42.29 (7.67)	40.59 (10.22)
	HGRE	102.63 (3.90)	99.27 (7.59)	100.92 (13.64)	93.95 (13.49)
	SRLGE	89.95 (27.58)	107.05 (16.48)	37.83 (11.03)	33.87 (15.84)
	SRHGE	108.95 (11.45)	108.42 (6.74)	109.96 (11.38)	112.03 (9.86)
	LRLGE	164.12 (7.60)	165.56 (7.45)	166.29 (4.53)	167.17 (5.03)
	LRHGE	114.83 (20.20)	126.48 (22.77)	113.47 (21.80)	126.18 (21.52)
	GLNU	36.25 (11.63)	45.63 (13.87)	38.77 (17.15)	56.06 (18.69)
	RLNU	84.41 (17.07)	98.13 (6.35)	99.18 (12.08)	110.37 (13.24)
	RPC	81.75 (9.55)	86.91 (10.91)	84.37 (12.74)	91.91 (15.21)

<https://doi.org/10.1371/journal.pone.0178843.t002>

for a specific patient and different spatial resolutions showing their wide range of variation as a function of the dynamic range.

### Experiment 2. Consistency of textural features and dynamic ranges for varying spatial resolutions

Next, for each textural feature, patient and dynamic range, we computed the CV for the four spatial resolutions considered. The CM entropy was the outstanding feature and the only robust feature for every dynamic range observed (Table 3). Only a low dynamic range (16-gray level) homogeneity was also robust.

Textural features dependence of different image reconstruction parameters is shown in Fig 3.

### Discussion

The analysis of texture parameters is a useful way of increasing the information obtainable from medical images.

This is a promising field of research, with applications ranging from the detection of lesions to differentiation between pathological and healthy tissue in different organs and the segmentation of anatomical structures. Texture analysis uses radiological images obtained in routine diagnostic practice, but involves an ensemble of mathematical computations performed with the data contained within the images. [1]

In oncology, there is an increasing evidence that texture analysis has the potential to augment diagnosis and characterization as well as improve tumor staging and therapy response assessment in oncological practice [2].

Different textural features, tumors and imaging modalities have been considered in the literature for cancer detection [5, 6], response to treatment [30] and survival group prediction [31]. However, the robustness of these methods under changes on 3D spatial resolution and dynamic range has not received much attention in brain MR imaging, being more popular in

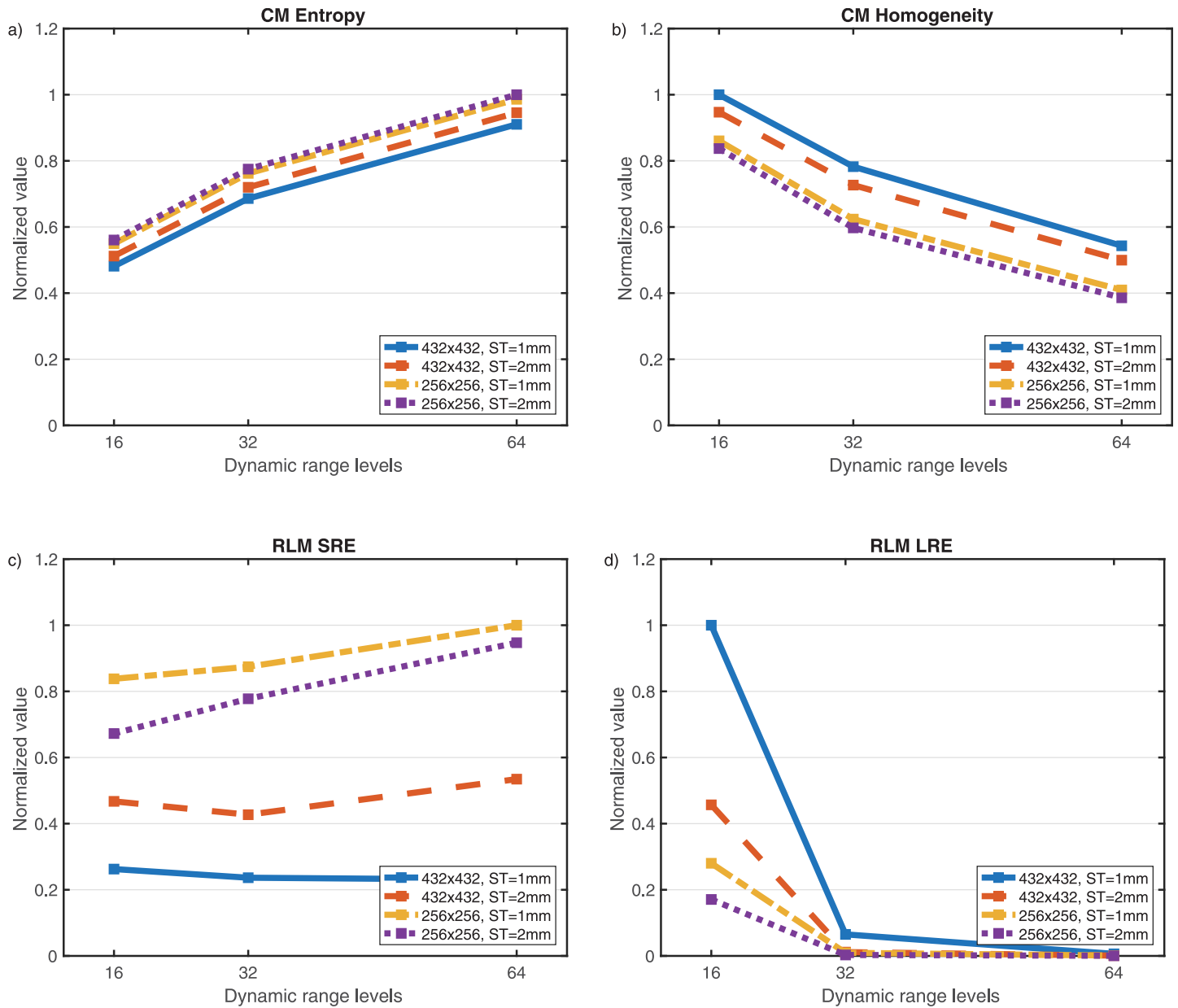


**Fig 2. Values of several textural features (normalized to the maximum value obtained in each subplot) for different spatial resolutions (432x432 ST 1mm, 432x432 ST 2 mm, 256x256 ST 1 mm, 256x256 ST 2 mm) and dynamic range values (16, 32 and 64 grey levels). Shown are results for a) co-occurrence (CM) Entropy, b) CM Homogeneity, c) run-length matrix (RLM) SRE, d) RLM LRE.**

<https://doi.org/10.1371/journal.pone.0178843.g002>

PET imaging [16, 32, 33]. In our study, none of the measures was robust under dynamic range changes, as it has been observed in limited 2D studies [17]. Thus, even at high spatial resolution, dynamic range substantially influences the textural measures' results.

Several works have employed CM and RLM based 2D features, using varied distances and directions between pixels, leading to large sets of 'different' measures [25, 29, 30]. However, in brain tumor imaging this workflow is meaningless, since patients are not explored exactly in the same positions, so different pixel distributions are compared using this methodology. Also, tumors are 3D structures, where study of their parameters in all the 3D directions is

**Table 3. Mean (and standard deviation) of the CV of the 20 patients' regarding each dynamic range considered.** CV was computed for each feature considering different combinations of matrix size and slice thickness, that is, matrix sizes of 432x432 and 256x256 pixels and slice thickness of 1 mm and 2 mm. Shaded cells correspond to those combinations obtaining a CV below 10%.

		Dynamic range		
		16 levels	32 levels	64 levels
Co-occurrence matrix	Entropy	7.91 (3.77)	6.31 (2.80)	5.08 (2.31)
	Homogeneity	7.13 (2.43)	10.89 (3.45)	13.96 (4.25)
	Contrast	38.94 (6.14)	44.40 (7.07)	46.86 (7.54)
	Dissimilarity	25.65 (5.15)	25.53 (4.79)	25.89 (4.97)
	Uniformity	19.54 (8.71)	21.94 (10.11)	23.15 (10.24)
Run-length matrix	LRE	108.66 (23.59)	125.03 (17.88)	117.39 (15.24)
	SRE	55.06 (28.39)	54.62 (14.88)	56.25 (14.71)
	LGRE	37.11 (6.70)	63.38 (12.02)	80.97 (11.96)
	HGRE	21.06 (5.48)	33.53 (6.34)	32.39 (6.40)
	SRLGE	65.82 (13.17)	85.34 (11.65)	97.96 (8.49)
	SRHGE	47.17 (34.13)	37.49 (18.52)	40.76 (15.56)
	LRLGE	90.24 (25.33)	107.14 (26.26)	89.65 (29.62)
	LRHGE	117.18 (20.80)	130.42 (14.57)	123.10 (12.52)
	GLNU	33.43 (7.44)	30.67 (12.23)	24.34 (7.24)
	RLNU	77.45 (23.39)	83.84 (15.30)	81.46 (13.09)
	RPC	44.25 (8.36)	58.03 (8.57)	58.12 (10.24)

<https://doi.org/10.1371/journal.pone.0178843.t003>

encouraged and would lead to a better characterization of tumor heterogeneity [20]. Reproducibility and robustness assessment are instigated in all fields of imaging and radiomics [34].

Previous findings imply, as long textural features should be used in clinical practice, that dynamic range has to be fixed in order to compare different studies. Its optimal threshold depends on the requisites of imaging analysis [16]. A dynamic range of 8 grey levels has been discouraged due to an insufficient contrast range resolution [35]. On the other hand, if the dynamic range is too large, many close grey-level values would be separated into different regions. Thus, we recommend acquiring either 16 or 32 different grey levels as dynamic range.

In any case, the very concept of identification of spatial structures by their closeness in an arbitrary 'uniform' grey level scale is one of the major weaknesses of RLM-based features, whatever is the number of grey levels taken.

As to the spatial resolution, we used only high resolution brain tumor scans in line with recent recommendations [36]. Thus, inconsistency of textural parameters is due to their lack of robustness.

Only the CM entropy was robust under spatial variations in our analysis. This feature is one of the most relevant textural measures and has been reported to have a predictive value in GBM patients [37], to distinguish radiation necrosis from metastasis in brain non-small cell lung cancer oligometastasis [38]. In other imaging settings, CM entropy was able to differentiate among breast cancer subtypes [39], in non-small cell lung cancers undergone to concomitant chemoradiotherapy [40] and between malignant and inflammatory pulmonary nodules [41]. In spite of its relevance, the fact that the remaining 15 measures studied were not robust, focus on their self-limitations as image complexity descriptors. These shortcomings are shared with PET textural analysis [32].

One would expect properly defined measures to be only weakly dependent—or no dependent at all—on the spatial discretization parameters. At least, they should converge to certain limit values when both the dynamic range and/or the spatial resolutions are sufficiently high. This is not the case for the measures studied here. We choose the RLM and CM measures

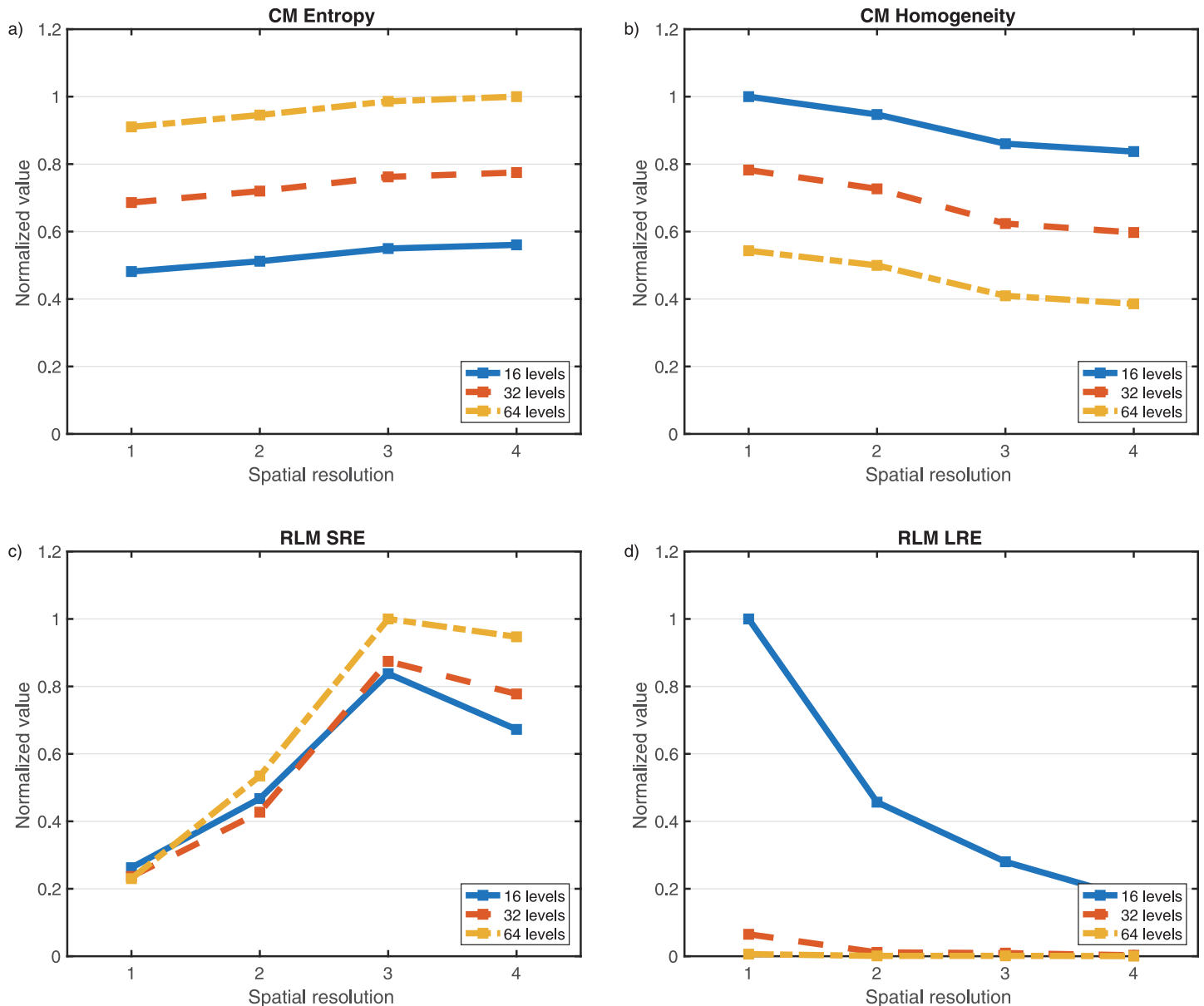


**Fig 3. Values of several textural features (normalized to the maximum value obtained in each subplot) for different dynamic range values (16, 32 and 64 grey levels) and spatial resolutions (432x432 ST 1mm, 432x432 ST 2mm, 256x256 ST 1mm, 256x256 ST 2mm). Shown are results for a) CM Entropy, b) CM Homogeneity, c) RLM SRE, d) RLM LRE.**

<https://doi.org/10.1371/journal.pone.0178843.g003>

because of their widespread use in oncological image-based studies either as individual predictors or as ‘imaging genes’ in the context of radiomics.

On the basis of our results there is a need for standardization of the spatial resolution if these measures are to be used in clinical practice. Most current images can be registered at a matrix size of 256x256. As to the slice thickness it should be fixed to 1 mm with 0 mm gap. This provides typically voxels of volume around 1 mm<sup>3</sup> [36].

This study has some advantages over previous works. First, to the best of our knowledge, robustness analysis under spatial resolution and grey-level changes has not been performed in brain tumor MR imaging. Secondly, our study used standard MR contrast-enhanced

T1-weighted sequences (CE-T1WI). Also, we used normalized textural measures definitions [32].

As to the potential limitations of our study, we have to point out the synthetic nature of our methodology: we decided to use one T1 sequence and use the Matlab software to generate three additional sequences from it. Another option could have been to submit patients to four different MRIs with different image parameters. However, that procedure would be susceptible to patient's movement artifacts, contrast-enhancement decay along time or other external variations. On the other hand, interpolation methods have shown their effectiveness, thus not changing substantially image information and reducing such possible artifacts [42]. Second, we did not compare T1-weighted sequences among different vendors. It may happen that early assumptions of good compatibility in textural analysis in multicenter studies irrespective of the scanner and acquisition parameters were too optimistic [43, 44]. Another limitation is that we only dealt with certain textural features, but we choose the most meaningful ones that are also those more used in the literature. Also, we only showed the robustness of CE-T1WI sequence, and other imaging sequences could be also analyzed [45].

In this work, the variations of textural features due to different imaging protocols using postcontrast pretreatment 3D CE-T1WI were assessed. The displayed lack of robustness lies in the nature of the measures considered and not on the specific sequence, however it could be interesting to analyze the variability of the measures using other imaging sequences such as 3D FLAIR.

The results found here go beyond of neuro-oncology setting and suggest that textural feature analysis of oncological images should be done carefully if results from different scanners/resolutions/dynamic ranges are to be compared. Also, while there are other types of textural features, such as those of spectral type [1, 10], most used parameters share such limitations. This fact raises the need for the development of additional families of texture descriptors, less dependent on matrix size and/or dynamic range.

## Conclusions

We have performed a wide analysis of the robustness of usual 3D textural features regarding different matrix sizes and dynamic range configurations. Results achieved show that 3D textural feature values depend substantially on the dynamic range, thus it is mandatory to fix it in order to obtain reliable and comparable results. After fixing the dynamic range, the CM Entropy was the only robust textural measure under spatial discretization changes. Due to the lack of robustness of the other measures, their use to assess heterogeneity in multi-center studies has to be standardized. As practical recommendations for brain tumor images we recommend using 16 levels of gray as dynamic range and resampling higher resolution images to 256x256 as matrix size corresponding typically to 1 mm voxels.

## Acknowledgments

The authors declare no competing financial interests.

## Author Contributions

**Conceptualization:** DM JPB AMG JM CV EA VM PG.

**Data curation:** DM JPB JM CV.

**Formal analysis:** DM JPB VM PG.

**Funding acquisition:** VM PG.

**Investigation:** DM JPB JM CV.

**Methodology:** DM JPB AMG JM CV EA VMGP.

**Project administration:** EA VMGP.

**Resources:** JM CV VMGP.

**Software:** DM JPB.

**Supervision:** EA VMGP.

**Visualization:** DM.

**Writing – original draft:** DM EA VMGP.

**Writing – review & editing:** DM JPB AMG JM CV EA VMGP.

## References

1. Castellano G, Bonilha L, Li LM & Cendes F. Texture analysis of medical images. *Clin. Radiol.* 2004; 59:1061–1069. <https://doi.org/10.1016/j.crad.2004.07.008> PMID: 15556588
2. Davnall F, Yip CS, Ljungqvist G, Selmi M, Ng F, Sanghera B, et al. Assessment of tumor heterogeneity: an emerging imaging tool for clinical practice? *Insights Imaging.* 2012; 3:573–589. <https://doi.org/10.1007/s13244-012-0196-6> PMID: 23093486
3. Alic L, Niessen WJ, Veenland JF. Quantification of Heterogeneity as a Biomarker in Tumor Imaging: A Systematic Review. *PLOS One.* 2014; 9:e110300. <https://doi.org/10.1371/journal.pone.0110300> PMID: 25330171
4. Kumar V, Gu Y, Basu S, Berglund A, Eschrich SA, Schabath MB, et al. Radiomics: the process and the challenges. *Magn. Reson. Imaging.* 2012; 30:1234–1248. <https://doi.org/10.1016/j.mri.2012.06.010> PMID: 22898692
5. Ellingson BM. Radiogenomics and imaging phenotypes in glioblastoma: novel observations and correlation with molecular characteristics. *Curr. Neurol. Neurosci. Rep.* 2015; 15:506. <https://doi.org/10.1007/s11910-014-0506-0> PMID: 25410316
6. Ginsburg SB, Alghohary A, Pahwa S, Gulani V, Ponsky L, Aronen HJ, et al. Radiomic features for prostate cancer detection on MRI differ between the transition and peripheral zones: preliminary findings from a multi-institutional study. *J Magn Reson Imaging.* 2016; in press. <https://doi.org/10.1002/jmri.25562> PMID: 27990722
7. Just N. Improving tumour heterogeneity MRI assessment with histograms. *Br. J. Cancer* 2014; 111:2205–2213. <https://doi.org/10.1038/bjc.2014.512> PMID: 25268373
8. Haralick RM, Shanmugam K, Dinstein I. Textural features for image classification. *IEEE Trans. Syst. Man. Cybern.* 1973; 6:610–621.
9. Galloway MM. Texture analysis using grey level run lengths. *Comp Graphics Image Processing.* 1975; 4:172–179.
10. Kassner A, Thornhill RE. Texture analysis: a review of neurologic MR imaging applications. *Am. J. Neuroradiol.* 2010; 31:809–816. <https://doi.org/10.3174/ajnr.A2061> PMID: 20395383
11. Larroza A, Moratal D, Paredes-Sánchez A, Soria-Olivas E, Chust ML, Arribas LA, et al. Support vector machine classification of brain metastasis and radiation necrosis based on texture analysis in MRI. *J Magn Reson Imaging.* 2015; 42:1362–1368. <https://doi.org/10.1002/jmri.24913> PMID: 25865833
12. Brooks FJ. On some misconceptions about tumor heterogeneity quantification. *Eur. J. Nucl. Med. Mol. Imaging.* 2013; 40:1292–1294. <https://doi.org/10.1007/s00259-013-2430-y> PMID: 23632962
13. Mayerhoefer ME, Szomolanyi P, Jirak D, Materka A, Trattnig S. Effects of MRI acquisition parameter variations and protocol heterogeneity on the results of texture analysis and pattern discrimination: an application-oriented study. *Med Phys.* 2009; 36:1236–1243. <https://doi.org/10.1118/1.3081408> PMID: 19472631
14. Waugh SA, Lerski RA, Bidaut L, Thompson AM. The influence of field strength and different clinical breast MRI protocols on the outcome of texture analysis using foam phantoms. *Med. Phys.* 2011; 38:5058–5066. <https://doi.org/10.1118/1.3622605> PMID: 21978050
15. Collewet G, Strzelecki M, Mariette F. Influence of MRI acquisition protocols and image intensity normalization methods on texture classification. *Magn. Reson. Imag.* 2004; 22:81–91.

16. Leijenaar RTH, Nalbantov G, Carvalho S, van Elmpt WJ, Troost EG, Boellaard R, et al. The effect of SUV discretization in quantitative FDG-PET Radiomics: the need for standardized methodology in tumor texture analysis. *Sci Rep*. 2015; 5:11075. <https://doi.org/10.1038/srep11075> PMID: 26242464
17. Molina D, Pérez-Beteta J, Martínez-González A, Martino J, Velásquez C, Arana E, et al. Influence of grey-level and space discretization on brain tumor heterogeneity measures obtained from magnetic resonance images. *Comp Med Biol*. 2016; 78:49–57.
18. Mahmoud-Ghoneim D, Toussaint G, Constans JM, de Certaines JD. Three dimensional texture analysis in MRI: a preliminary evaluation in gliomas. *Magn. Reson. Imaging*. 2003; 21:983–987. PMID: 14684200
19. Arai K, Herdiyeni Y, Okumura H. Comparison of 2D and 3D Local Binary Pattern in Lung Cancer Diagnosis. *Int. J. Adv. Comp. Sci. & Appl*. 2012; 3:4. <https://doi.org/10.14569/IJACSA.2012.030416>
20. Depeursinge A, Foncubierta-Rodriguez A, Van De Ville D, Müller H. Three-dimensional solid texture analysis in biomedical imaging: Review and opportunities. *Med. Image Anal*. 2014; 18:176–196. <https://doi.org/10.1016/j.media.2013.10.005> PMID: 24231667
21. Georgiadis P, Cavouras D, Kalatzis I, Glotsos D, Athanasiadis E, Kostopoulos S, et al. Enhancing the discrimination accuracy between metastases, gliomas and meningiomas on brain MRI by volumetric textural features and ensemble pattern recognition methods. *Magn Reson Imaging*. 2009; 27:120–130. <https://doi.org/10.1016/j.mri.2008.05.017> PMID: 18602785
22. Mahmoud-Ghoneim D, Toussaint G, Constans JM, de Certaines JD. Three dimensional texture analysis on MRI: a preliminary evaluation in gliomas. *Magn Reson Imaging*. 2013; 21:983–987.
23. Pérez-Beteta J, Martínez-González A, Molina D, Amo-Salas M, Luque B, Arregui E, et al. Glioblastoma: does the pre-treatment geometry matter? A postcontrast T1 MRI-based study. *Eur Radiol*. 2016. <https://doi.org/10.1007/s00330-016-4453-9> PMID: 27329522
24. Molina D, Pérez-Beteta J, Luque B, Arregui E, Calvo M, Borrás JM, et al. Tumour heterogeneity in glioblastoma assessed by MRI texture analysis: a potential marker of survival. *Br. J. Radiol*. 2016; 89:20160242.
25. Ganeshan B, Abaleke S, Young RCD, Chatwin CR, Miles KA. Texture analysis of non-small cell lung cancer on unenhanced computed tomography: initial evidence for a relationship with tumour glucose metabolism and stage. *Cancer imaging*. 2010; 10:137–143. <https://doi.org/10.1102/1470-7330.2010.0021> PMID: 20605762
26. Kurani, AS, Xu DH, Furst J, Raicu DS. Co-occurrence Matrices for Volumetric Data. The In 7th IASTED International Conference on Computer Graphics and Imaging. 2004.
27. Galloway MM. Texture analysis using grey level run lengths. *Comp. Graphics Image Process*. 1975; 4:172–179.
28. Xu DH, Kurani AS, Furst JD, Raicu DS. Run-length encoding for volumetric texture. *Heart*. 2004; 27:25–30.
29. Reed GF, Lynn F, Meade BD. Use of coefficient of variation in assessing variability of quantitative assays. *Clin. Diagn. Lab. Immunol*. 2002; 9:1235–1239. <https://doi.org/10.1128/CDLI.9.6.1235-1239.2002> PMID: 12414755
30. Liu J, Mao Y, Li Z, Zhang D, Zhang Z, Hao S, et al. Use of texture analysis based on contrast-enhanced MRI to predict treatment response to chemoradiotherapy in nasopharyngeal carcinoma. *J Magn Reson Imaging*. 2016; 44:445:455. <https://doi.org/10.1002/jmri.25156> PMID: 26778191
31. Zhou M, Chaudhury B, Hall LO, Goldgof DB, Gillies RJ, Gatenby RA. Identifying spatial imaging biomarkers of glioblastoma multiforme for survival group prediction. *J Magn Reson Imaging*. 2016; in press. <https://doi.org/10.1002/jmri.25497> PMID: 27678245
32. Orlhac F, Soussan M, Maisonobe JA, Garcia CA, Vanderlinden B, Buvat I. Tumor Texture Analysis in 18F-FDG PET: Relationships Between Texture Parameters, Histogram Indices, Standardized Uptake Values, Metabolic Volumes, and Total Lesion Glycolysis. *J. Nucl. Med*. 2014; 55:414–422. <https://doi.org/10.2967/jnumed.113.129858> PMID: 24549286
33. Buvat I, Orlhac F, Soussan M. Tumor Texture Analysis in PET: Where Do We Stand? *J. Nucl. Med*. 2015; 56:1642–1644. <https://doi.org/10.2967/jnumed.115.163469> PMID: 26294296
34. Yip SS, Aerts HJ. Applications and limitations of radiomics. *Phys Med Biol*. 2016; 61:R150–66. <https://doi.org/10.1088/0031-9155/61/13/R150> PMID: 27269645
35. Tixier F, Hatt M, Le Rest CC, Le Pogam A, Corcos L, Visvikis D. Reproducibility of tumor uptake heterogeneity characterization through textural feature analysis in 18F-FDG PET imaging. *J. Nucl. Med*. 2012; 53:693–700. <https://doi.org/10.2967/jnumed.111.099127> PMID: 22454484
36. Ellingson BM, Bendzus M, Boxerman J, Barboriak D, Erickson BJ, Smits M, et al. Consensus recommendations for a standardized Brain Tumor Imaging Protocol in clinical trials. *Neur Oncol*. 2015; 17:1188–1198.

37. Lee J, Jain R, Khalil K, Griffith B, Bosca R, Rao G, et al. Texture Feature Ratios from Relative CBV Maps of Perfusion MRI Are Associated with Patient Survival in Glioblastoma. *Am. J. Neuroradiol.* 2016; 37:37–43. <https://doi.org/10.3174/ajnr.A4534> PMID: 26471746
38. Nardone V, Tini P, Boindi M, Sebaste L, Vanzi E, De Otto G, et al. Prognostic Value of MR Imaging Texture Analysis in Brain Non-Small Cell Lung Cancer Oligo-Metastases Undergoing Stereotactic Irradiation. *Cureus.* 2016; 25:e584. <https://doi.org/10.7759/cureus.584> PMID: 27226944
39. Waugh SA, Purdie CA, Jordan LB, Vinnicombe S, Lerski RA, Martin P, et al. Magnetic resonance imaging texture analysis classification of primary breast cancer. *Eur Radiol.* 2016; 26:322–330. <https://doi.org/10.1007/s00330-015-3845-6> PMID: 26065395
40. Ahn SY, Park CM, Park SJ, Kim HJ, Song C, Lee SM, et al. Prognostic Value of Computed Tomography Texture Features in Non-Small Cell Lung Cancers Treated With Definitive Concomitant Chemoradiotherapy. *Invest Radiol.* 2015; 50:719–725. <https://doi.org/10.1097/RLI.000000000000174> PMID: 26020832
41. Suo S, Cheng J, Cao M, Lu Q, Yin Y, Xu J, et al. Assessment of Heterogeneity Difference Between Edge and Core by Using Texture Analysis: Differentiation of Malignant From Inflammatory Pulmonary Nodules and Masses. *Acad Radiol.* 2016; 23:1115–1122. <https://doi.org/10.1016/j.acra.2016.04.009> PMID: 27298058
42. Luk-Pat GT, Nishimura DG. Reducing off-resonance distortion by echo-time interpolation. *Magn. Reson. Med.* 2001; 45:269–276. PMID: 11180435
43. Herlidou-Meme S, Constans JM, Carsin B, Olivie D, Eliat PA, Nadal-Desbarats L, et al. MRI texture analysis on texture test objects, normal brain and intracranial tumors. *Magn Reson Imaging.* 2003; 21:989–993. PMID: 14684201
44. Lu L, Ehmke RC, Schwartz LH, Zhao B. Assessing agreement between radiomic features computed for multiple CT imaging settings. *PLOS One.* 2016; 9:e166550. <https://doi.org/10.1371/journal.pone.0166550> PMID: 28033372
45. Assefa D, Keller H, Ménard C, Laperriere N, Ferrari RJ, Yeung I. Robust texture features for response monitoring of glioblastoma multiforme on T1-weighted and T2-FLAIR MR images: A preliminary investigation in terms of identification and segmentation. *Med Phys.* 2010; 37:1722–1736. <https://doi.org/10.1118/1.3357289> PMID: 20443493